J Nanopart Res (2019) 21: 107
https://doi.org/10.1007/s11051-019-4532-3

RESEARCH PAPER

# Reliable quantitative SERS analysis mediated by Ag nano coix seeds with internal standard molecule

**Yixiang Xu · Hongmei Liu · Tao Jiang**

Received: 19 December 2018 / Accepted: 16 April 2019 / Published online: 23 May 2019


**Abstract** Nanostructure with an interior nanogap has received much attention in surface-enhanced Raman scattering (SERS). However, controllable synthesis of nanostructure with ultrasmall nanogap and innovative morphology still remains a challenge. Herein, we present a facile seed-mediated route to integrate uniform nanogap in novel Ag nano coix seeds and locate Raman molecules in the nanogap at room temperature. After 20-nm Ag nanoparticles (NPs) modified by Raman ligand 2-naphthalenethiol and coated by polymer shells as cores were obtained, outside Ag shells were formed by in situ reduction on the polymer surface. The SERS properties of these resulting Ag nano coix seeds were systematically explored. More importantly, the novel SERS active substrate exhibited ultrahigh homogeneity, reproducibility, stability, and even a reliable quantitative SERS analysis mediated by internal standard molecules.

**Keywords** Nanogap · Nano coix seed · Inbuilt Raman molecule · Surface-enhanced Raman scattering · Instrumentation

## Introduction

Surface-enhanced Raman scattering (SERS), combining superior sensitivity, in situ detection ability, exceptional spectral selectivity, and fingerprint features, has stimulated widespread interest ranging from chemical analysis (Lin et al. 2017; Yan et al. 2016), immunoassay (Banaei et al. 2017; Jiang et al. 2018a, b), and food safety (Gillibert et al. 2018) to environmental monitoring (Yang et al. 2016; Chamuah et al. 2017). The high sensitivity of SERS is usually obtained by confining Raman reporters within the range of electromagnetic field, which is originated from the localized surface plasmon resonance (LSPR) of noble metal nanomaterials (Schider et al. 1999; Jensen et al. 2000; Willets and Duyne 2007). It is well known that resonant property depends strongly on size, morphology, and structure of nanomaterials, besides the environmental dielectric constant (Kelly et al. 2003; David et al. 2011; Jiang et al. 2016; Kang et al. 2013). Thereafter, these confined electromagnetic fields, terminated as "hot spots," are usually achieved by constructing versatile nanomaterials with ultrasmall gap (Zhao et al. 2017), sharp tip (Li et al. 2014), or rough surface (Zou et al. 2018). Particularly, great efforts have been made to develop novel core-shell nanostructures which possess high SERS activity in the past decades. For example,

**Electronic supplementary material** The online version of this article (https://doi.org/10.1007/s11051-019-4532-3) contains supplementary material, which is available to authorized users.

Y. Xu · T. Jiang (✉)
Department of Microelectronic Science and Engineering, Institute of Photonics, Faculty of Science, Ningbo University, Ningbo 315211, People's Republic of China
e-mail: jiangtao@nbu.edu.cn

H. Liu (✉)
Institute of Solid State Physics, Shanxi Datong University, Datong, Shanxi 037009, People's Republic of China
e-mail: lhm9898@163.com

core-shell Au nanostructure with an ultrasmall interior nanogap of about 1 nm was constructed by using thiolated DNA and obtained an enhancement factor greater than $1.0 \times 10^8$ (Lim et al. 2011). Ultrathin Ag layer was deposited on Au core to form a core-shell structure with embedded 4-mercaptobenzoic acid molecule for enhancing SERS signal from bare Ag nanoparticles (NPs) (20 times stronger) (Feng et al. 2012). Triangular Ag@Au nanoplates were reported to exhibit considerably enhanced SERS performance compared to the bare Ag nanoplates due to the hot spots emerging at their sharpened edges and nanogaps located between Ag cores and Au shells (Liu et al. 2015). Although several monodisperse core-shell nanostructures have been successfully created by these methods (Kumar-Krishnan et al. 2017; Jiang et al. 2017a, b, c), it is still a challenge to synthesize well-defined ones with novel morphology and controlled distribution for reproducible and stable ultrasensitive assay.

In the past decades, the development of SERS technique encountered two main barriers (Cardinal et al. 2017; Li et al. 2017). The first one is the obtaining of a substrate with a large amount of electromagnetic hot spots, which can be partially resolved by designing core-shell nanostructures as discussed above (Zhang et al. 2018). The second one is how to place the targeted molecules exactly on or in the obtained hot spots (Jiang et al. 2017a, b, c). Recently, an ultrathin shell around the noble metal NPs was prepared using polystyrene-block-poly(acrylic acid) (PSPAA). Raman reporter on the surface of noble metal NPs can be effectively protected without dissociation for a long store period. Simultaneously, the inert polymer shell would not affect the output of SERS signals (Yang et al. 2009; Chen et al. 2010).

With large scattering to extinction cross-section ratio, Ag NPs have sensitive LSPR. Thus, they are more competitive in plasmonic sensing and SERS applications (Dmitruk et al. 2010). However, the successful preparation of Ag NPs with uniform size and shape in aqueous solution remains very challenging. Recently, the seed-mediated solution–phase growth technique has become an effective and versatile method to prepare noble metal NPs (Jiang et al. 2017a, b, c; Yao et al. 2017). Nonetheless, little attention has been paid to the construction of a well-defined seed with uniform geometry size for the preparation of novel core-shell nanostructures using a seed-mediated strategy.

Herein, we designed a facile, rapid, and reproducible three-step route to realize the synthesis of novel Ag nano coix seeds with SERS-active ligand in the interior gaps. Ag NPs with a coix seed-like shape were prepared through the growth of an outside Ag layer on the Ag@PSPAA core with built-in Raman ligand (2-naphthalenethiol, 2NT) by in situ reduction. Time-dependent experiment was carried out to confirm the coating process. Notably, these Ag nano coix seeds exhibit remarkably improved SERS activity, good reproducibility, and longtime stability attributed to the well-defined interior polymer gap as well as the uniform size and shape of the nano coix seeds. The minimum concentration detected for 2NT was 0.00624 mM with a wide linear range from 62.4 to 0.00624 mM. The homogeneity of the SERS signal was subsequently investigated and relative standard deviation (RSD) values of only 12.17%, 9.99%, and 10.85% for 1069, 1382, and 1624 $cm^{-1}$ peaks of 2NT were obtained, respectively. The signal reproducibility of the Ag nano coix seeds prepared by the same method was also evaluated and RSD value of about 15% was achieved for 5 pitches of samples. The stability of the SERS signal for more than 2 weeks was then confirmed. Finally, a reliable quantitative SERS analysis of 4-nitrothiophenol (4NTP) in solution was realized using the 2NT in Ag nano coix seeds as the internal standard to represent and eliminate the environment fluctuation. The simple seed-mediated strategy to prepare nano coix seeds and exactly locate the Raman molecules into their interior gaps provides new opportunities to create diverse and novel SERS substrates for various applications.

## Experimental

### Chemicals

Hydrogen tetrachloroaurate(III) hydrate ($HAuCl_4 \cdot xH_2O$, 99.9%) was purchased from Alfa Aesar. Sodium borohydride ($NaBH_4$), sodium citrate, $AgNO_3$, L-ascorbic acid, NaCl, 2NT, DMF, and hydroxylamine were obtained from Sigma-Aldrich. Amphiphilic diblock copolymer PSPAA ($PS_{154}$–*b*–$PAA_{49}$) was purchased from Polymer Source. Deionized water (> 18.2 MΩ $cm^{-1}$) was used throughout the experiment.

### Sample preparation

Synthesis of 20-nm Ag NPs and encapsulating them with PSPAA have been reported in our previous work (Jiang et al. 2018a, b). In a typical synthesis, the 20-nm Ag NPs, 2NT molecules, and PSPAA were mixed in the solution of DMF and $H_2O$, where the DMF/$H_2O$ volume ratio was 4.5. The mixture was heated to 110 °C for 2 h and then cooled down to room temperature. Finally, the product was collected by centrifugation and the 2NT molecules were encapsulated into the PSPAA shell. The DMF/$H_2O$ volume ratio and heating temperature are both very important factors in the encapsulation process.

Synthesis of Ag nano coix seeds: 1 mL aqueous solution of above Ag@PSPAA NP was mixed with 9 mL aqueous solution of 6 mg sodium citrate, 4 mg ascorbic acid, and 0.94 mg NaCl. And then, 2 mL aqueous solution of $AgNO_3$ (1 mg/mL) was added dropwise into the precursor solution with stirring for 1 h. Finally, the product was collected by centrifugation at 8000 rpm for 10 min. The typical synthesis process of the Ag nano coix seeds is schematically illustrated in Scheme 1.

Preparation of the Ag nano coix seeds SERS substrate: a silica wafer (about 1 $cm^2$) was pretreated with $O_2$ plasma for 10 min to improve its surface hydrophilicity. The wafer was then functionalized with an amino group by reacting with APTES solution (5 mM) for 1 h. Subsequently, the wafer was soaked in citrate-stabilized Ag nano coix seed solution for 2 h to ensure the adsorption of Ag NPs and rinsed with $H_2O$ twice to remove the excess NPs.

### Instrumentation

The morphologies of the products were observed and analyzed by a SU70 field emission scanning electron microscopy (FESEM) and a JEM1400 transmission electron microscopy (TEM). The optical absorption spectra of the products were recorded with a Cary 100 ultraviolet-visible (UV-vis) spectrophotometer. The SERS properties of the samples were examined by a miniature Raman spectrometer (BWS415, B&W Tek Inc.) using a 785-nm semiconductor laser as an excitation source. The laser power on the targeted position was 20 mW and the accumulation time was 5 s. All the analyses were performed at room temperature.

## Result and discussion

In a typical synthesis, novel Ag nano coix seeds were successfully prepared with high yield by dropwise adding an aqueous solution of $AgNO_3$ into the precursor solution containing ascorbic acid, sodium citrate, NaCl, and the above core-shell seeds (size of core 20 ± 5 nm, size of shell 10 ± 3 nm, Fig. S1). Figure 1a and b show the typical SEM images of the resulting Ag NPs. These images clearly indicate that an interesting morphology appears: one side of the Ag NP is round and the other side is sunken with a small opening. Such morphology is similar to that of coix seeds, a Chinese medicine as exhibited in the inset of Fig. 1a. Therefore, the as-prepared Ag nanostructure was defined as "Ag nano coix seeds." The distribution histogram of the diameter of the Ag nano coix seeds is illustrated in Fig. 1c, which exhibits a mean value of 90 ± 5 nm with a relatively narrow distribution range from 60 to 140 nm. In the typical TEM images of the Ag nano coix seeds, subtle cores and gaps between cores and shells can be seen in nearly all the NPs after careful identification (Fig. 1d). The central core and gap can be certified after amplifying the image of a typical Ag nano coix seed (Fig. 1e). The mean gap size was estimated to be approximately 4.2 to 9.7 nm. HRTEM image collected from the Ag nano coix seed (Fig. 1f) clearly displays d-spacing (111) of 0.24 nm (the length of ten lattices is 2.4 nm), which is consistent with its corresponding selected-area electron diffraction (SAED) pattern. The diffraction pattern exhibits bright spots of a sixfold symmetry corresponding to the {220} reflections of the fcc Ag single crystal orientated in the [111] direction (Fig. 1g), which arises from the modification of sodium citrate on the surface of the Ag nano coix seeds. This is further supported by the energy-dispersive spectrum (EDS) of the Ag NPs as shown in Fig. 1h. Besides the peaks of Ag from the NPs and Cu from the substrates, the peak of C from sodium citrate and PSPAA also appears. In Fig. 1i, the local elemental mapping of these Ag nano coix seeds clearly exhibits the spatial distribution of the Ag element. The chemical state of Ag nano coix seeds was also examined using XPS. The binding energies of Ag $^3d_{5/2}$ and Ag $^3d_{3/2}$ were identified as 368.2 and 374.2 eV, respectively (Fig. 1j). The spin energy separation of 6.0 eV indicated a zero valence state of the Ag NPs (Gang et al. 2003). As introduced above, the LSPR of Ag NPs depends strongly on their size, shape, and structure as well as on the environmental dielectric constant. In the typical three-

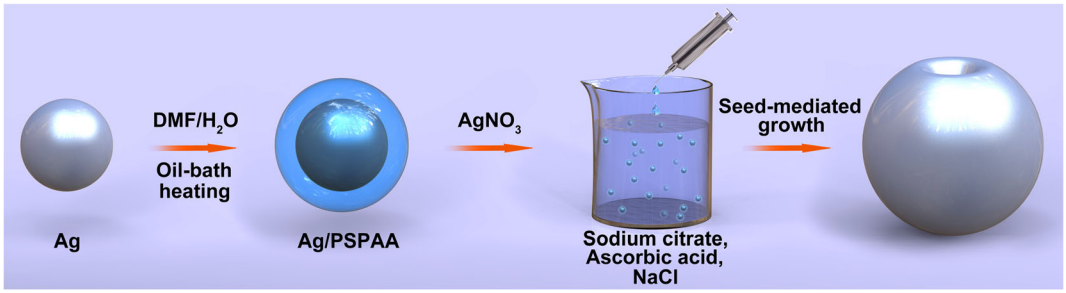


**Scheme 1** Schematic illustration of the three-step synthesis of Ag nano coix seeds

step synthesis process, an obvious red-shift and broadening of the absorption band of Ag NPs was observed as illustrated in Fig. 1k. The absorption peak of the Ag NPs shifts from 402 to 436 nm after they were coated by the block copolymers with a higher refractive index. With the further coating of the second grown Ag layer, the absorption band of NPs becomes broadened significantly and a second main peak further appears at 532 nm with a shoulder at 343 nm.

The corresponding growth process of the outside Ag layer has been monitored as illustrated in Fig. 2a to c. It can be explained as follows: the precursor complex of

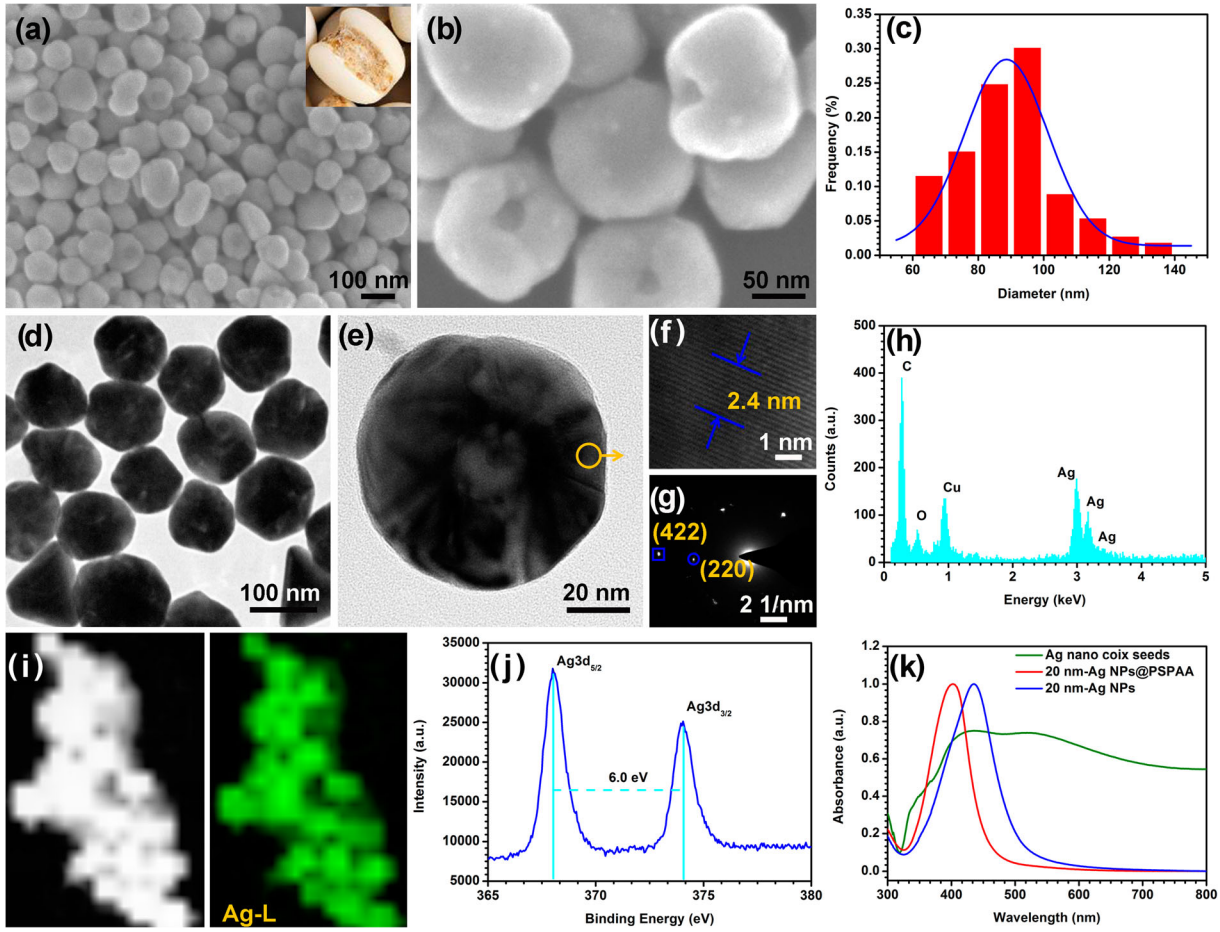


**Fig. 1** **a**, **b** SEM images, **c** diameter distribution, **d**, **e** TEM images, **f** HRTEM image, **g** SAED pattern, **h** EDS, **i** local elemental mapping, **j** XPS, and **k** absorption spectra of the Ag nano coix seeds. The inset of **a** is the photograph of the real coix seeds. There are also absorption spectra of 20-nm Ag NPs and 20-nm Ag NPs@PSPAA in **k**

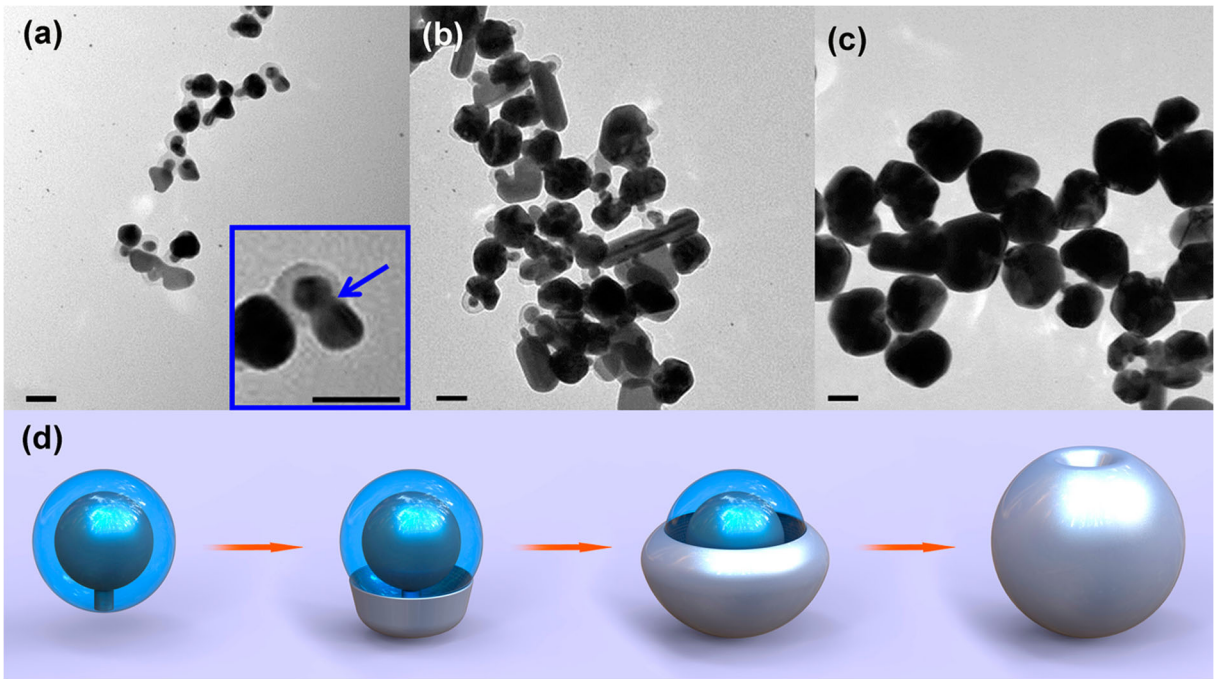


**Fig. 2** TEM images of the products at different reaction periods: **a** 15, **b** 30, and **c** 60 min and **d** the corresponding growth mechanism (scale bar 50 nm)

carboxyl group and $Ag^+$ was established through cationic interactions when $AgNO_3$ was slowly dripped into the precursor solution. Then, $Ag^+$ was gradually released from the complex and reduced to $Ag^0$ under the effect of ascorbic acid. The Ag atoms would diffuse into the porous PSPAA shell and nucleated on the surface of inner Ag NPs (Mai and Eisenberg 2012). This is an energy-favored process compared to homogeneous nucleation in the growth solution or heterogeneous nucleation on the surface of a polymer shell. As a result, the low concentration of Ag atoms around the Ag surface promoted the single-site heterogeneous nucleation (Feng et al. 2017). After that, Ag nuclei penetrated the polymer shell and eventually grew out of the shell, forming a "bridge" (as being pointed out by the arrows in Fig. 1e and in the inset of Fig. 2a). After attaching more newly appeared Ag nuclei in the solution, they progressively grew to small Ag particles and were temporarily stabilized by the excess surfactant citrate molecules. These initial Ag particles acted as seeds and grew large gradually across the polymer shell, with the synergistic effect of NaCl selectively etching twinned seeds (Wiley et al. 2004; Long et al. 2014). As is reported, the defects inherent in twinned nuclei of silver would provide active sites for their selective etching and dissolution by chloride and oxygen from air, leaving only the single crystalline ones to grow into nanoparticles (Wiley et al. 2004). Finally, a small opening will be observed in the final nanostructures, probably owing to the dislocation of the growth ends and the high combing energy barrier. The proper growth mechanism of the sample was shown in Fig. 2d. Therefore, the seeded strategy developed in this work gives rise to constructing novel Ag nano coix seeds with ultrasmall inner gaps.

After the Ag nano coix seed SERS substrates were carefully prepared as shown in Fig. 3a, the representative SERS spectra of the Ag nano coix seeds were collected in Fig. 3b. These spectra showed several prominent peaks at 522, 603, 639, 770, 845, 1069, 1382, 1453, 1570, 1587, and 1624 $cm^{-1}$, corresponding to the characteristic peak positions of 2NT (Jiang et al. 2018a, b; Puebla et al. 2004). As the dilution of the target molecules, the SERS intensity gradually dropped and it was even possible to identify the peak of 2NT with the trace amount of 0.00624 mM, which was the minimum concentration detected. Also, a linear dependence between the SERS intensity at 1069 $cm^{-1}$ and the 2NT amount from 0.00624 to 62.4 mM was confirmed after linear fitting, and a relationship as $I = 4417.94 \cdot \mathrm{LogC} + 10{,}984.86$ was given (Fig. 3c). This superior detection performance of the as-prepared Ag nano coix seeds

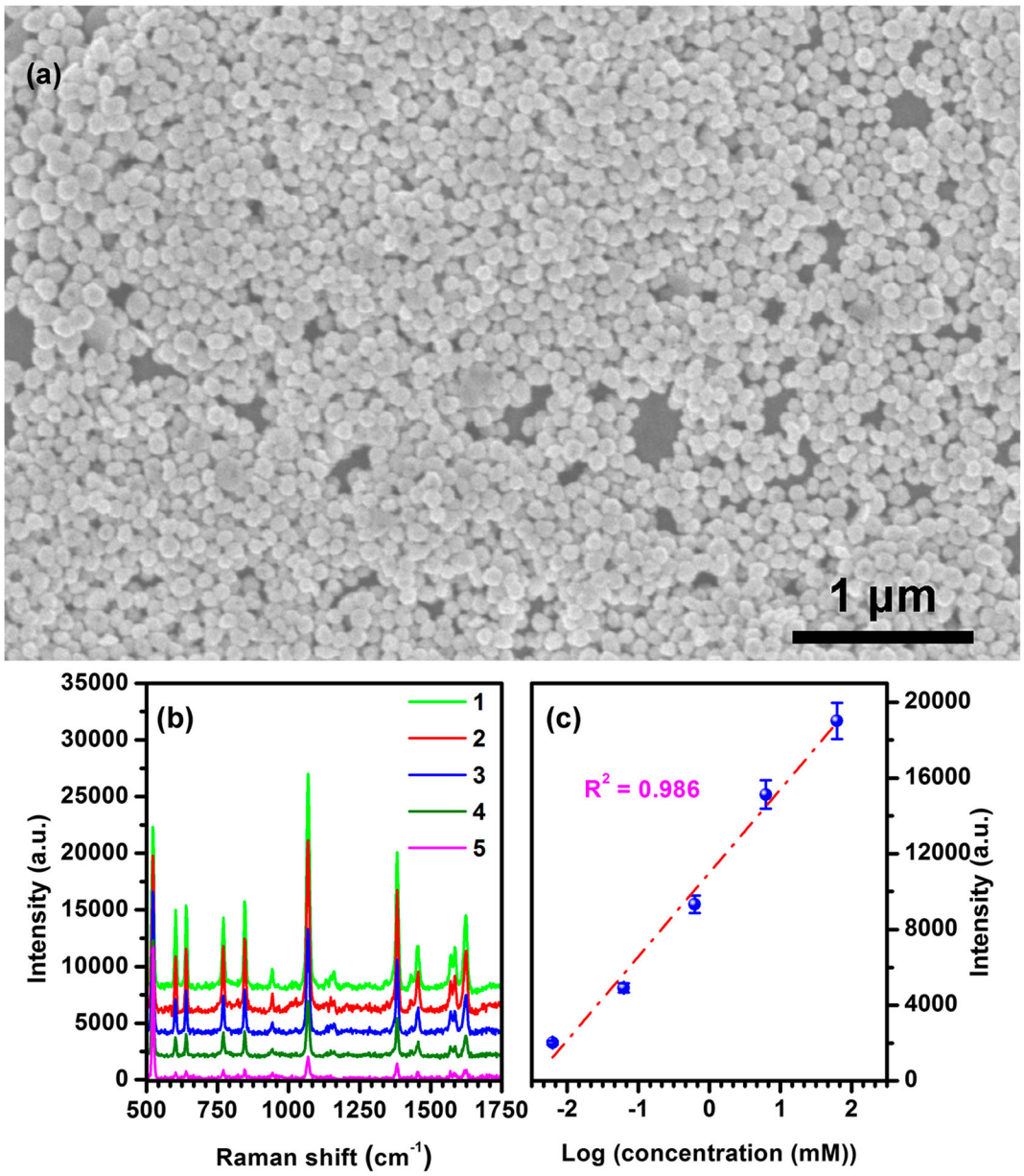


**Fig. 3** **a** SEM image of Ag nano coix seed-modified substrate. **b** SERS spectra of the Ag nano coix seeds loaded with different amounts of 2NT (62.4 (1), 6.24 (2), 0.624 (3), 0.0624 (4), and 0.00624 (5) mM) and **c** the corresponding calibration curve

arose from the highly electromagnetic hot spots, which were induced by the efficient plasmonic coupling between the external Ag layers and the inner Ag NPs. The signal reproducibility of the Ag nano coix seeds was then investigated, and the resulting 2D color-coded intensity of the spatiotemporal SERS mapping of 2NT from 20 randomly selected probe sites was depicted in Fig. 4a. From 500 to 1750 $cm^{-1}$, the characteristic Raman vibrations of 2NT were obviously enhanced at all spots, indicating excellent SERS activity and homogeneity. The RSD values of the intensity of three main SERS peaks at 1069, 1382, and 1624 $cm^{-1}$ were then calculated as 12.17% (Fig. 4b), 9.99% (Fig. S2a), and 10.85% (Fig. S2b), evidencing the homogeneity of Raman enhancement. As shown in the above SEM and TEM images, the existence of nanogaps in nearly all the Ag nano coix seeds can induce a wide distribution of the SERS hot spots on the NP-modified substrate and the

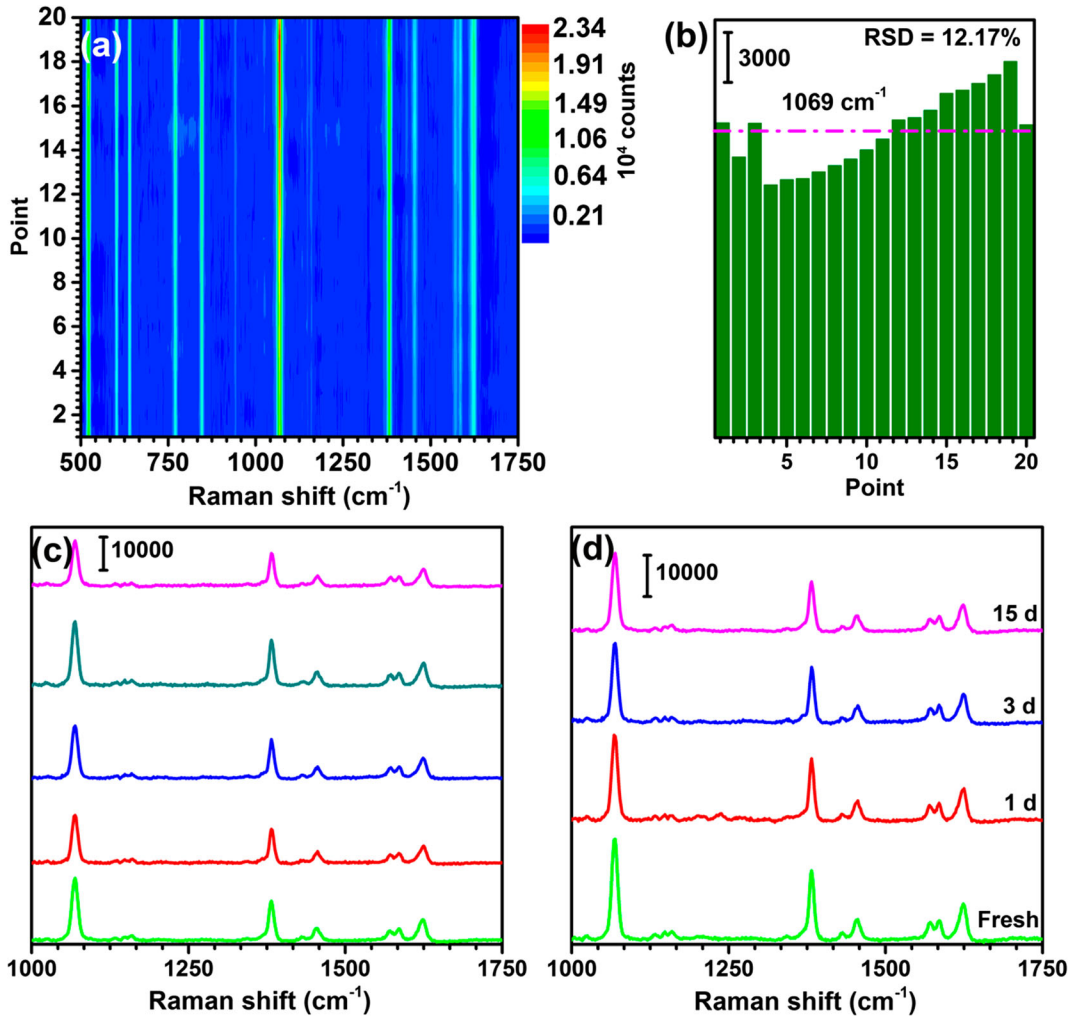


**Fig. 4** **a** The 2D color-coded intensity of spatiotemporal SERS mapping and **b** the SERS intensities of 2NT molecules at 1069 $cm^{-1}$ from the Ag nano coix seeds. **c** SERS spectra of 2NT from five different batches of the Ag nano coix seeds and **d** temporal stability of the SERS signal

exact location of the 2NT molecules in these hot spots promoted the appearance of the homogeneous SERS output. Moreover, the narrow size distribution and relatively uniform shape of the Ag nano coix seeds can also contribute to the homogeneity of SERS signals.

To visualize the SERS reproducibility of the Ag nano coix seeds provided by repeated synthesis, the Raman spectra of 2NT measured from different batches of samples were recorded in Fig. 4c. All characteristic peaks in the Raman spectra gave slight oscillations, demonstrating the reproducibility of these SERS nanostructures. The RSD values of SERS intensity were calculated to be 15.51%, 13.23%, and 12.96% for peaks at 1069, 1382, and 1624 $cm^{-1}$, respectively. The high reproducibility of the SERS signals with a RSD value of around 15% can be attributed to the effective repetitive preparation of the nanostructures, which was favored by the simplicity of the seed-mediated technique. The temporal stability of the Ag nano coix seed SERS substrate, which is an essential factor in practical assay, was also investigated. The SERS intensity of 2NT was gradually reduced by about 20% of the initial intensity in the following day and then maintained at a similar intensity for the next 2 weeks as shown in Fig. 4d. In this study, the Raman ligand was encapsulated on the surface of the inner Ag layer and protected by the polymer shell. Compared with the conventional surface modification strategies, the present method avoided the dissociation

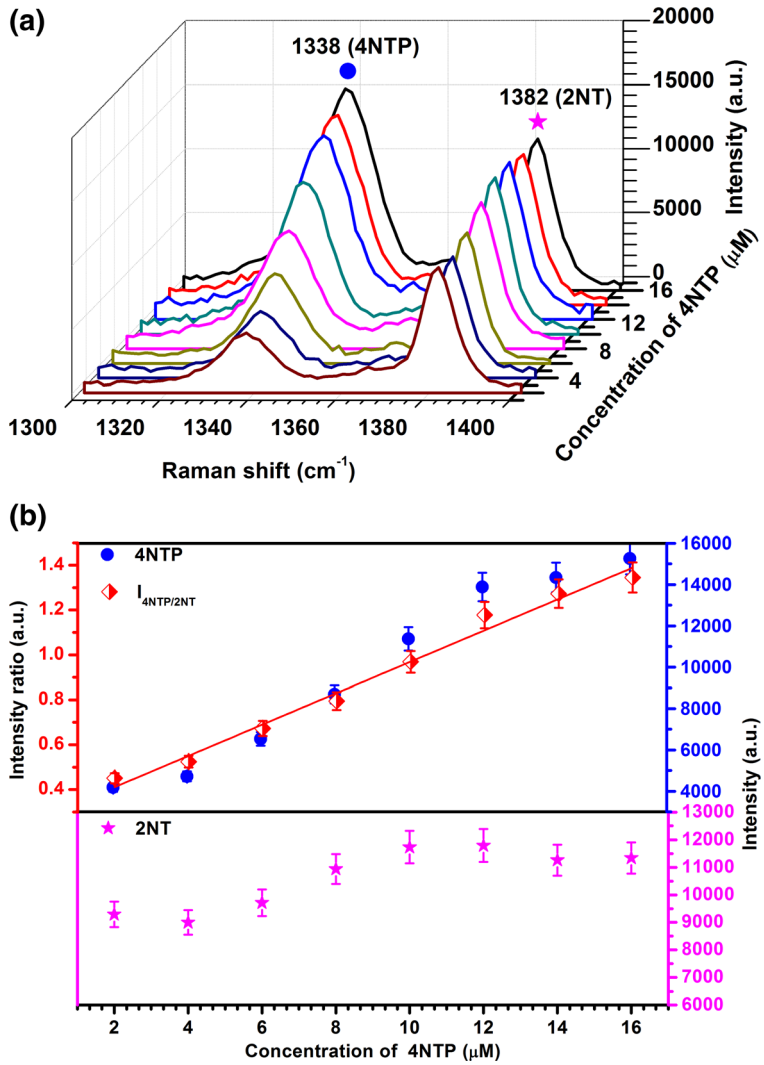


**Fig. 5** **a** SERS spectra of 4NTP (target) and 2NT (internal standard) and **b** SERS intensities of the target 4NTP (1338 $cm^{-1}$), 2NT (1382 $cm^{-1}$), and relative intensities of 1338 to 1382 $cm^{-1}$ at various 4NTP concentrations

and random distribution of target Raman molecules. Consequently, their exact and right positions in the special geometric-constructed hot spots led to a more uniform and reliable output of SERS signals.

Both the interior gap with exactly located molecules and the high SERS activity of the as-prepared nanostructure would provide its versatile abilities. As it is previously reported, reliable quantitative SERS analysis can be facilitated by core-shell NPs with embedded internal standards (Shen et al. 2015). The signal of the embedded Raman probe (2NT) in the Ag nano coix seeds will represent the fluctuation and interference of environment such as solution conditions. When other target molecules were detected, its SERS signal can be corrected by considering and disposing the basic signal from the inner 2NT. Such a strategy was demonstrated by using 4NTP as targeted molecules. The SERS spectra were collected from the solution of the Ag nano coix seeds modified by 4NTP (Fig. 5a), and the signal intensity of 4NTP fluctuates with the dilution of the solution (Fig. 5b, top panel, solid circle). Consequently, a poor linear relationship was observed, which is due to the gradual aggregation of Ag nano coix seeds induced by the addition of 4NTP. Such an aggregation was reflected by the gradually increasing SERS intensity of 2NT (internal standard; Fig. 5b, down panel, solid star). Interesting and excitingly, the linear relationship between the SERS intensity and the concentration of the molecules from 2 to 16 μM can be improved by normalizing the SERS intensity of 4NTP (1338 $cm^{-1}$) to that of 2NT (1382 $cm^{-1}$) as shown in Fig. 5b (top panel, open diamond). A possible reason is that such a normalization based on the internal standard

may represent and eliminate the influence from the external environment (mainly aggregation induced by the additive ligand in the solution). As a consequence, it is demonstrated that the Ag nano coix seeds with internal standard molecules can serve as an ideal platform for quantitative SERS analysis.

## Conclusions

In conclusion, a facile seed-mediated route was introduced to integrate interior ultrasmall gap with the size of about 10 nm in novel Ag nano coix seeds. Temporal experiment was directed to confirm the coating processes of outside Ag shells. The detection limitation of 2NT molecule located exactly in the gap was 0.00624 mM with a wide linear range from 62.4 to 0.00624 mM. The homogeneous SERS performance of the Ag nano coix seeds with RSD values of around 10% was subsequently confirmed by the spatiotemporal SERS mapping. The SERS reproducibility of the samples produced by five parallel experiments was also evaluated and RSD value of about 15% was obtained for different characteristic peaks. Particularly, the stability of SERS signal was certified to be good after being stored for more than 2 weeks. Finally, a reliable quantitative SERS analysis was realized by using the 2NT molecules in the Ag nano coix seeds as an internal standard to eliminate the influence from external environment.

**Funding information** This work was supported by the Natural Science Foundation of Zhejiang Province (Grant no. LY19F050002), the Natural Science Foundation of Ningbo (Grant No. 2018A610316), the Applied Basic Research Project of Shanxi Province (Grant No. 201701D221096), and K.C. Wong Magna Fund in Ningbo University, China.

**Compliance with ethical standards**

**Conflict of interest** The authors declare that they have no conflict of interest.

## References

Banaei N, Foley A, Houghton JM, Sun YB, Kim B (2017) Multiplex detection of pancreatic cancer biomarkers using a SERS-based immunoassay. Nanotechnology 28:455101

Cardinal MF, Ende EV, Hackler RA, McAnally MO, Stair PC, Schatz GC, Duyne RPV (2017) Expanding applications of SERS through versatile nanomaterials engineering. Chem Soc Rev 46:3886–3903

Chamuah N, Chetia L, Zahan N, Dutta S, Ahmed GA, Nath P (2017) A naturally occurring diatom frustule as a SERS substrate for the detection and quantification of chemicals. J Phys D Appl Phys 50:175103

Chen G, Wang Y, Yang MX, Xu J, Goh SJ, Pan M, Chen HY (2010) Measuring ensemble-averaged surface-enhanced Raman scattering in the hotspots of colloidal nanoparticle dimers and trimers. J Am Chem Soc 132:3644–3645

David C, Guillot N, Shen H, Toury T, de la Chapelle ML (2011) SERS detection of biomolecules using lithographied nanoparticles towards a reproducible SERS biosensor. Nanotechnology 21:475501

Dmitruk NL, Malynych SZ, Moroz IE, Kurlyak VY (2010) Optical efficiency of Ag and Au nanoparticles. Semicond Phys Quantum Electron Optoelectron 13:369–373

Feng YH, Wang Y, Wang H, Chen T, Tay YY, Yao L, Yan QY, Li SZ, Chen HY (2012) Engineering "hot" nanoparticles for surface-enhanced Raman scattering by embedding reporter molecules in metal layers. Small 8:246–251

Feng YH, Wang YW, Song XH, Xing SX, Chen HY (2017) Depletion sphere: explaining the number of Ag islands on Au nanoparticles. Chem Sci 8:430–436

Gang L, Anderson BG, van Grondelle J, van Santen RA (2003) Low temperature selective oxidation of ammonia to nitrogen on silver-based catalysts. Appl Catal B Environ 40:101–110

Gillibert R, Triba MN, de la Chapelle ML (2018) Surface enhanced Raman scattering sensor for highly sensitive and selective detection of ochratoxin A. Analyst 143:339–345

Jensen TR, Malinsky MD, Haynes CL, Duyne RPV (2000) Nanosphere lithography: tunable localized surface plasmon resonance spectra of silver nanoparticles. J Phys Chem B 104:10549–10556

Jiang T, Wang XL, Zhou J, Chen D, Zhao ZQ (2016) Hydrothermal synthesis of Ag@$MSiO_2$@Ag three core–shell nanoparticles and their sensitive and stable SERS properties. Nanoscale 8:4908–4914

Jiang T, Wang XL, Tang SW, Zhou J, Gu CJ, Tang J (2017a) Seed-mediated synthesis and SERS performance of graphene oxide-wrapped Ag nanomushroom. Sci Rep 7:9795

Jiang T, Wang XL, Tang J, Zhou J, Gu CJ, Tang SW (2017b) The seeded-synthesis of core–shell Au dumbbells with inbuilt Raman molecules and their SERS performance. Anal Methods 9:4394–4399

Jiang T, Wang XL, Zhou J (2017c) The synthesis of four–layer gold–silver–polymer–silver core–shell nanomushroom with inbuilt Raman molecule for surface–enhanced Raman scattering. Appl Surf Sci 426:965–971

Jiang T, Wang XL, Tang J, Tang SW (2018a) Seed-mediated synthesis of floriated Ag nanoplates as surface enhanced Raman scattering substrate for in situ molecular detection. Mater Res Bull 97:201–206

Jiang T, Wang XL, Zhou J, Jin H (2018b) The construction of silver aggregate with inbuilt Raman molecule and gold nanowire forest in SERS-based immunoassay for cancer biomarker detection. Sensors Actuators B Chem 258:105–114

Kang LL, Xu P, Zhang B, Tsai H, Han XJ, Wang HL (2013) Laser wavelength- and power-dependent plasmon-driven chemical reactions monitored using single particle surface enhanced Raman spectroscopy. Chem Commun 49:3389–3391

Kelly KL, Coronado E, Zhao LL, Schatz GC (2003) The optical properties of metal nanoparticles: the influence of size, shape, and dielectric environment. J Phys Chem B 107:668–677

Kumar-Krishnan S, Estevez-Gonz'alez M, P'erez R, Esparza R, Meyyappan M (2017) A general seed-mediated approach to the synthesis of AgM (M = Au, Pt, and Pd) core–shell nanoplates and their SERS properties. RSC Adv 7:27170–27176

Li JP, Zhou J, Jiang T, Wang BB, Gu M, Petti L, Mormile P (2014) Controllable synthesis and SERS characteristics of hollow sea-urchin gold nanoparticles. Phys Chem Chem Phys 16: 25601–25608

Li P, Yan XN, Zhou F, Tang XH, Yang LB, Liu JH (2017) A capillary force-induced Au nanoparticle–Ag nanowire single hot spot platform for SERS analysis. J Mater Chem C 5: 3229–3237

Lim DK, Jeon KS, Hwang JH, Kim H, Kwon S, Suh YD, Nam JM (2011) Highly uniform and reproducible surface-enhanced Raman scattering from DNA-tailorable nanoparticles with 1-nm interior gap. Nat Nanotechnol 6:452–460

Lin KQ, Yi J, Zhong JH, Hu S, Liu BJ, Liu JY, Zong C, Lei ZC, Wang X, Aizpurua J, Esteban R, Ren B (2017) Plasmonic photoluminescence for recovering native chemical information from surface-enhanced Raman scattering. Nat Commun 8:14891

Liu HP, Liu TZ, Zhang L, Han L, Gao CB, Yin YD (2015) Etching-free epitaxial growth of gold on silver nanostructures for high chemical stability and plasmonic activity. Adv Funct Mater 25:5435–5443

Long R, Zhou S, Wiley BJ, Xiong YJ (2014) Oxidative etching for controlled synthesis of metal nanocrystals: atomic addition and subtraction. Chem Soc Rev 43:6288–6310

Mai YY, Eisenberg A (2012) Self-assembly of block copolymers. Chem Soc Rev 41:5969–5985

Puebla RAA, Santos DSJD, Aroca RF (2004) Surface–enhanced Raman scattering for ultrasensitive chemical analysis of 1 and 2–naphthalenethiols. Analyst 129:1251–1256

Schider G, Gotschy W, Leitner A, Aussenegg FR (1999) Squeezing the optical near-field zone by plasmon coupling of metallic nanoparticles. Phys Rev Lett 82:2590–2593

Shen W, Lin X, Jiang CY, Li CY, Lin HX, Huang JT, Wang S, Liu GK, Yan XM, Zhong QL, Ren B (2015) Reliable quantitative SERS analysis facilitated by core–shell nanoparticles with embedded internal standards. Angew Chem Int Ed 54:7308–7312

Wiley B, Herricks T, Sun YG, Xia YN (2004) Polyol synthesis of silver nanoparticles: use of chloride and oxygen to promote the formation of single-crystal, truncated cubes and tetrahedrons. Nano Lett 4:1733–1739

Willets KA, Duyne RPV (2007) Localized surface plasmon resonance spectroscopy and sensing. Annu Rev Phys Chem 58: 267–297

Yan XN, Li P, Yang LB, Liu JH (2016) Time–dependent SERS spectra monitoring the dynamic adsorption behavior of bipyridine isomerides combined with bianalyte method. Analyst 141:5189–5194

Yang MX, Chen T, Lau WS, Wang Y, Tang QH, Yang YH, Chen HY (2009) Development of polymer–encapsulated metal nanoparticles as surface–enhanced Raman scattering probes. Small 5:198–202

Yang SK, Dai XM, Stogin BB, Wong TS (2016) Ultrasensitive surface-enhanced Raman scattering detection in common fluids. Proc Natl Acad Sci 113:268–273

Yao QF, Yuan X, Fung V, Yu Y, Leong DT, Jiang DE, Xie JP (2017) Understanding seed-mediated growth of gold nanoclusters at molecular level. Nat Commun 8:927

Zhang C, Lia CH, Yu J, Jiang SZ, Xu SC, Yang C, Liu YJ, Gao XG, Liu AH, Man BY (2018) SERS activated platform with three-dimensional hot spots and tunable nanometer gap. Sensors Actuators B Chem 258:163–171

Zhao Y, Li XY, Wang MS, Zhang LC, Chu BH, Yang CL, Liu Y, Zhou DF, Lu YL (2017) Constructing sub–10–nm gaps in graphene–metal hybrid system for advanced surface–enhanced Raman scattering detection. J Alloys Compd 720: 139–146

Zou J, Song W, Xie W, Huang B, Yang H, Luo Z (2018) A simple way to synthesize large-scale $Cu_2O$/Ag nanoflowers for ultrasensitive surface-enhanced Raman scattering detection. Nanotechnology 29:115703